

HRh[P(OPh)₃]₄ as a hydrogenation and isomerization catalyst

H.K.A.C. Coolen^a, R.J.M. Nolte^a, P.W.N.M. van Leeuwen^{b,*}

^a Nijmegen SON Research Center, Department of Organic Chemistry, University of Nijmegen, Toemooiveld, 6525 ED Nijmegen, Netherlands

^b J.H. van't Hoff Instituut, Department of Anorganic Chemistry, University of Amsterdam, Nieuwe Achtergracht 166, 1018 WV Amsterdam, Netherlands

Received 13 October 1994; in revised form 10 January 1994

Abstract

The preparation and reactions of [HRh[P(OPh)₃]₄] (**2**) have been investigated. The metallation product [(PhO)₂(C₆H₄OP)Rh[P(OPh)₃]₃] (**4**) has been characterized by ³¹P NMR spectroscopy. Catalytic hydrogenation of alkenes with **2** depends strongly on the amount of extra ligand added and the substrate (1-hexene, *Z,E*-2-hexene and allylbenzene). Without added phosphite, traces of [(HRh[P(OPh)₃]₂]₂] are the actual catalyst. Under these conditions the reaction is zero order in substrate. The kinetics are completely different when extra triphenyl phosphite is present. Complex **2** behaves as a catalyst with a character in between that of ClRh(PPh₃)₃ and cationic Rh(diphosphine)⁺.

Keywords: Rhodium; Hydrogenation catalyst; Isomerization catalyst

1. Introduction

The hydrogenation of alkenes by rhodium(I)-phosphine complexes is one of the most extensively examined reactions in homogeneous catalysis [1]. It involves the formation of a metal hydride by activation of molecular hydrogen, the migratory insertion of the hydride to a coordinated alkene and the hydrogenolysis of the metal alkyl species [2]. The sequence in which these processes take place are defined by the type of catalyst and the properties of the residual ligands on the metal center. The first step in the hydrogenation with the well-known “Wilkinson” catalyst [ClRh(PPh₃)₃] is the oxidative addition of molecular hydrogen to a coordinatively unsaturated complex. This step is followed by the coordination and the insertion of the alkene and finally the hydrogenolysis of the metal alkyl species [3]. Because of this sequence this mechanism is often referred to as the hydride path. In contrast with this route, the hydrogenation with ionic catalysts of the type [(solvent)₂Rh⁺(PR₃)₂] dominantly involves a so-called alkene path. The first step is the coordination of an alkene to a free site on the metal center, followed by oxidative addition of H₂, insertion and reductive elimi-

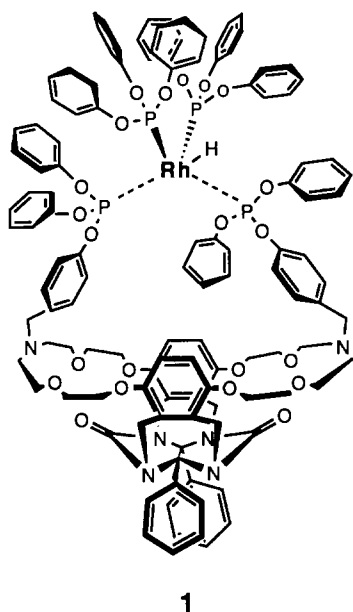
nation [3c,4]. Both catalysts are classified as “dihydride hydrogenation catalysts”. The way by which monohydride catalysts such as [HRh(CO)(PPh₃)₃] activate dihydrogen is much less understood, although in the consecutive reactions the same elementary steps are involved [5].

Metal complexes of triorganylphosphites are generally supposed to be inefficient hydrogenation catalysts, by reason of the putative high π acidity of the phosphite ligands. However, no detailed discussions have been presented in the literature which endorse and explain this assumption. To our knowledge only three hydrogenation catalysts based on phosphites have been reported [6,7].

Recently, we described a supramolecular catalyst consisting of a synthetic host molecule provided with a rhodium triarylphosphite complex (**1**). This catalyst is capable of selectively hydrogenating alkene substrates bound in its cavity [8]. In order to obtain more detailed information about the functioning of **1** we carried out a study on the corresponding catalyst without the substrate binding moiety.

In this paper we report the spectroscopic features and catalytic properties of [HRh[P(OPh)₃]₄] (**2**) as a hydrogenation and isomerization catalyst for 1-hexene and allylbenzene. We shall also present an alternative synthetic route for **2**. Although **2** appears not to be a

* Corresponding author.



versatile hydrogenation catalyst, details of its functioning can give further insight in the electronic influences of phosphites as ligands.

2. Results and discussion

2.1. Synthesis of $\text{HRh}[\text{P}(\text{OPh})_3]_4$

The preparation of **2** has been described in the literature. It involves the reaction of $[\text{HRh}(\text{CO})(\text{PPh}_3)_3]$ with an excess of triphenylphosphite [9]. Recently, an alternative route was reported starting from $[(\text{acac})\text{Rh}(\text{CO})_2]$ and $\text{P}(\text{OPh})_3$ [10]. Both routes are based on rhodium(I) complexes. We synthesized $[\text{HRh}[\text{P}(\text{OPh})_3]_4]$ directly from rhodium(III) chloride and triphenylphosphite with NaBH_4 in ethanolic solution, analogous to the preparation of $[\text{HCo}[\text{P}(\text{OPh})_3]_4]$ and $[\text{Ni}[\text{P}(\text{OPh})_3]_4]$ [9b]. To avoid transesterification of the phosphite ligands the reaction mixture was kept at 0°C . Once coordinated to a metal center the triphenylphosphite is protected against solvolysis [11].

2.2. Reactions of $\text{HRh}[\text{P}(\text{OPh})_3]_4$ in solution

Since the first report of **2** in the literature, many contradicting statements about its reactions in solution have been published [10,12]. Comparison of the various reports, combined with our own observations, encourages us to summarize the reactions of **2** as shown in Scheme 1.

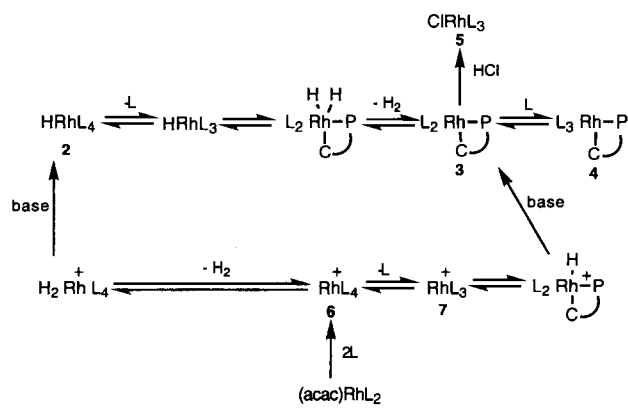
As can be seen from this scheme the ability to undergo orthometallation [13] is an important feature of **2** in solution. In this process an ortho aromatic C–H

bond is activated and oxidatively added to the rhodium center in an intramolecular fashion, resulting in a five-membered metallacycle. The first sequence of reactions, involving **2–4** was described by Parshall and coworkers [12a,12b]. These reactions explain the observed deuterium exchange of the *ortho* hydrogen atoms of the triphenylphosphite ligands. We found that after stirring a solution of **2** in CHCl_3 for 2 h under of D_2 at 5 bar, complete exchange was achieved, resulting in $[\text{DRh}\{\text{P}[\text{O}(2,6\text{-D}_2\text{C}_6\text{H}_3)]_3\}_4]$, as was confirmed by ^1H NMR and ^{31}P NMR spectroscopy. The addition of an excess of free phosphite reduces the rate of this process substantially, inhibiting the dissociation of a ligand from **2**.

Reaction of **3** with hydrochloric acid gives tris(triphenylphosphite) rhodium(I) chloride (**5**). This reaction involves the electrophilic attack of a proton on the rhodium center followed by reductive elimination which corresponds to the reverse of the metallation reaction.

Compound **6** was described in the literature long ago [12a,14]. Reaction of this compound with molecular hydrogen under influence of a base leads to the starting complex **2** [12a]. As mentioned before, **2** can be synthesized from $[(\text{acac})\text{Rh}(\text{CO})_2]$ (**8**) and triphenylphosphite [10]. The observation in the literature that **6** is formed in solution when **8** is treated with an excess of $\text{P}(\text{OPh})_3$ [12f] makes us to believe that the synthesis of **2** from **8** actually proceeds via **6**, the dissociated acetylacetonate anion probably acting as the base. Complex **6** can dissociate to form **7** [12a,12e]. We suggest also that **7** has the ability to undergo orthometallation to form **3** after deprotonation. This should explain the formation of **4** from **8** and $\text{P}(\text{OPh})_3$ in the absence of H_2 [12c].

With regard to the synthesis and characterization of **3** and **4**, conflicting reports exist concerning the number of residual phosphite ligands on the rhodium center. It is reported that **4** is formed by refluxing **2** or $[\text{HRh}(\text{CO})(\text{PPh}_3)_3]$ with $\text{P}(\text{OPh})_3$ in *n*-heptane [12b,15]. According to Borefield and Parshall [12a], **3** is prepared by reacting $[\text{ClRh}[\text{P}(\text{OPh})_3]_3]$ (**5**) with PhMgBr , fol-



Scheme 1.

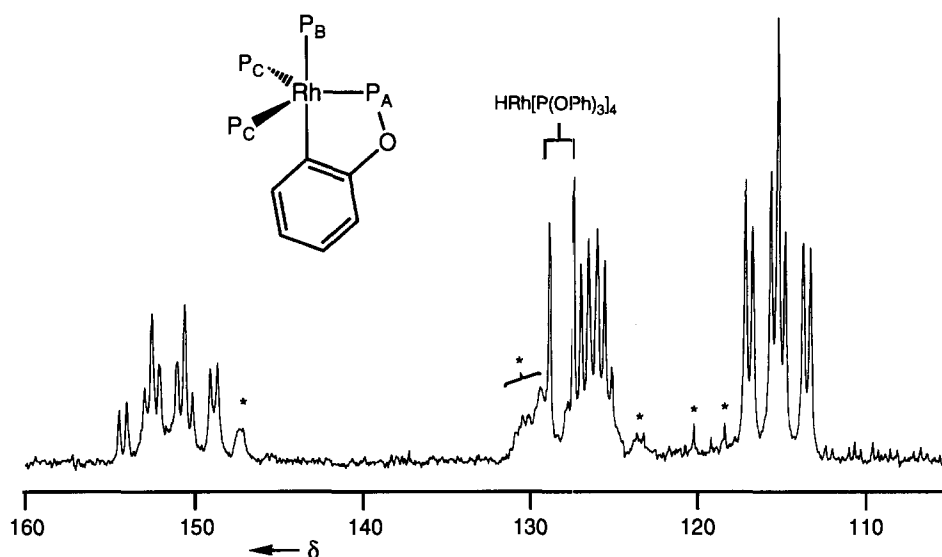


Fig. 1. The proposed structure and the $^{31}\text{P}\{^1\text{H}\}$ NMR spectrum in C_6D_6 (160 MHz) of **4**. The signals labelled with an asterisk are due to impurities.

lowed by the spontaneous reductive elimination of benzene. We re-examined these different literature procedures for **3** and **4** and submitted the products to a closer analysis. As it is known that the elimination of methane is a much faster process [16], we used MeMgCl instead of PhMgBr in the last-mentioned reaction. The main product from both syntheses could be identified as **4**, according to the ^{31}P NMR spectrum in C_6D_6 and IR spectroscopy. The IR spectra of both reaction products revealed the characteristic signals at $\tilde{\nu} = 800\text{ cm}^{-1}$ and 1010 cm^{-1} , assigned to the orthometallated complexes [12]. The ^{31}P NMR spectrum is shown in Fig. 1 and was simulated [17] to satisfy an ABC_2X pattern (A, B, C = ^{31}P ; X = ^{103}Rh) with $\delta(\text{A}) = 151.6\text{ ppm}$ ($J_{\text{Rh}-\text{P}(\text{A})}$

$= 236\text{ Hz}$, $J_{\text{P}(\text{A})-\text{P}(\text{B})} = 78\text{ Hz}$, $J_{\text{P}(\text{A})-\text{P}(\text{C})} = -314\text{ Hz}$), $\delta(\text{B}) = 126.3\text{ ppm}$ ($J_{\text{Rh}-\text{P}(\text{B})} = 159\text{ Hz}$, $J_{\text{P}(\text{B})-\text{P}(\text{C})} = 71\text{ Hz}$) and $\delta(\text{C}) = 115.3\text{ ppm}$ ($J_{\text{Rh}-\text{P}(\text{C})} = 236\text{ Hz}$). Other combinations of relative signs of the coupling constants also give fairly good fits, but $J_{\text{P}(\text{A})-\text{P}(\text{C})}$ and $J_{\text{P}(\text{B})-\text{P}(\text{C})}$ must have opposite relative signs. The phosphorus atom involved in the five-membered metallacycle (P_A) displays the expected shift of approximately 35 ppm to lower field with regard to the other phosphorus ligands in the equatorial plane [18]. The strong mutual coupling between the P atoms in this plane (314 Hz), which is somewhat larger than that of related hydride rhodium species [19], is remarkable. On account of these data we propose a trigonal bipyramidal structure of the complex

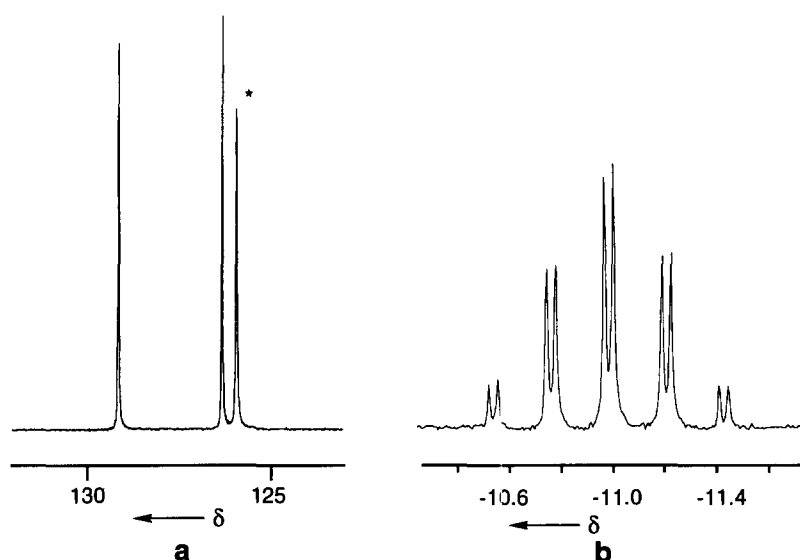


Fig. 2. (a) The 80 MHz $^{31}\text{P}\{^1\text{H}\}$ NMR spectrum and (b) the high field region of the 200 MHz ^1H NMR spectrum of $\text{HRh}[\text{P}(\text{OPh})_3]_4$ (**2**) in CDCl_3 . The signal labelled with an asterisk is due to free $\text{P}(\text{OPh})_3$.

as is shown in Fig. 1. A similar structure was assumed for the corresponding cobalt analog [7a]. From these results can be concluded that **3** cannot be isolated by way of these reaction procedures.

A tetrahedral arrangement of the phosphites around the rhodium center in **2** has been proposed on the basis that **2** is isomorphous with $[\text{HCo}[\text{P}(\text{OPh})_3]_4]$, $[\text{HNi}[\text{P}(\text{OPh})_3]_4]$ and $[\text{Pt}[\text{P}(\text{OPh})_3]_4]$, from the evidence of powder diffraction data. The hydride is positioned along one of the trigonal axes. However, in the $^{31}\text{P}\{^1\text{H}\}$ NMR spectrum of a solution of **2** in CDCl_3 , only one sharp doublet at $\delta = 127.7$ ppm ($J_{\text{Rh-P}} = 229$ Hz) is observed (Fig. 2(a)). The magnetic equivalence of the phosphorus atoms has been explained by a fast “tunneling” of the hydrogen atom around the edges of the tetrahedron [20]. Alternatively, it is known [19] that trigonal bipyramidal structures undergo extremely fast pseudo-Berry–Smith [21] rotations, thus making the phosphorus resonances equivalent on the NMR time scale. This is also ex-

pressed by the appearance of a well-defined doublet of quintets for the hydride signal in the high field region of the ^1H NMR spectrum of **2** (CDCl_3 ; $\delta = -11.0$ ppm; $J_{\text{H-P}} = 44$ Hz; $J_{\text{H-Rh}} = 7$ Hz) (Fig. 2(b)). The observed $J_{\text{H-P}} = 44$ Hz is the average of one large *trans* coupling constant and three smaller *cis* coupling constants with opposite signs.

Interestingly, the hydride signal of the corresponding phosphine complex $\text{HRh}(\text{PPh}_3)_4$ is strongly broadened and displays no fine structure; this is attributed to rapid ligand exchange [22].

3. Catalytic hydrogenation and isomerization

3.1. Results

To examine the behavior of **2** as a hydrogenation and isomerization catalyst we used 1-hexene and allylben-

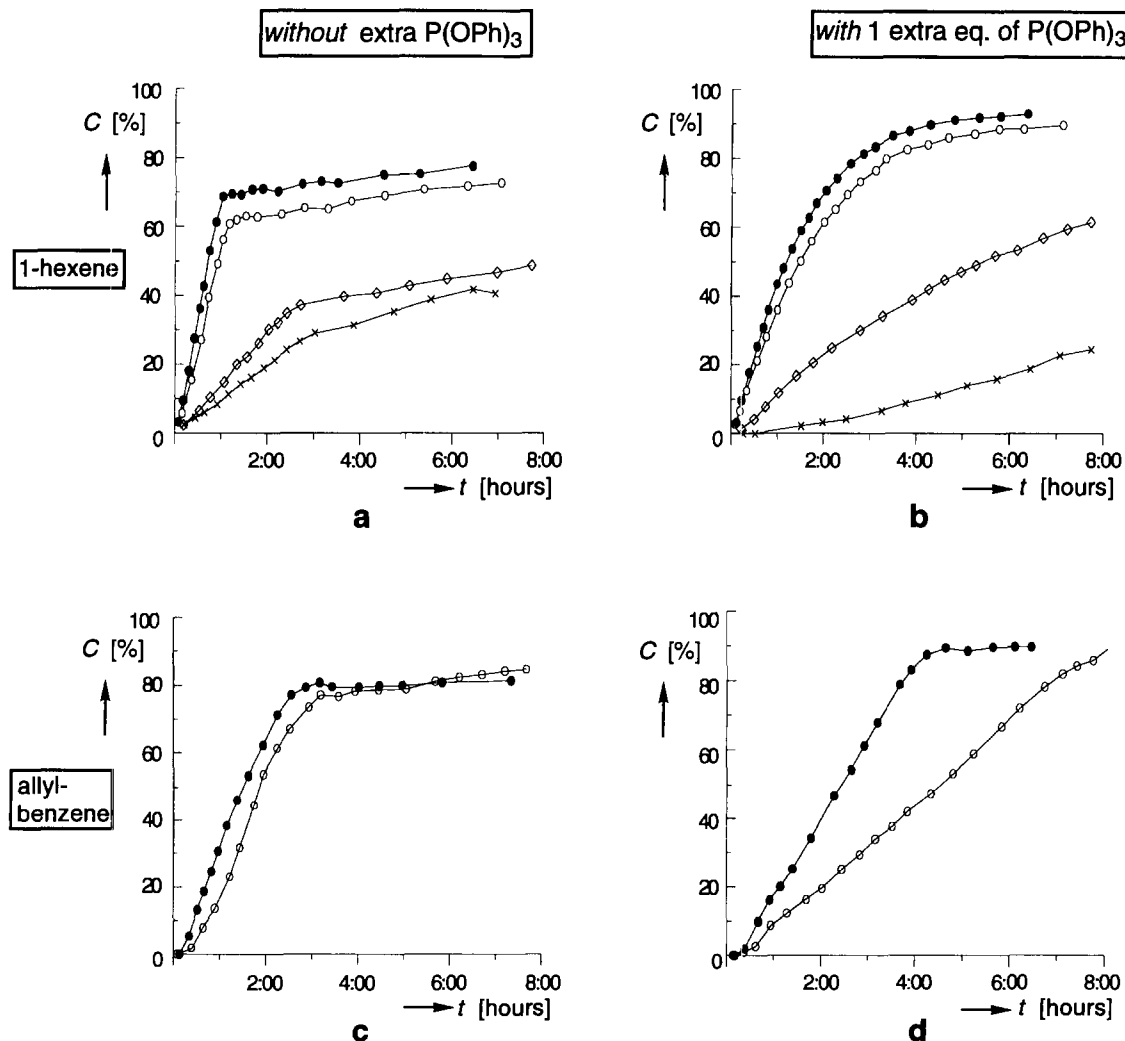


Fig. 3. The formation of (a), (b) hexane and (c), (d) propylbenzene in separate hydrogenation experiments of 1-hexene and allylbenzene by $\text{HRh}[\text{P}(\text{OPh})_3]_4$ (a), (c) without and (b), (d) with an additional equivalent of $\text{P}(\text{OPh})_3$ at 0.2 atm (x), 1.0 atm (◇), 5.0 atm (○) and 10 atm (●).

Table 1
Observations during hydrogenation and isomerization of alkenes by $\text{HRh}[\text{P}(\text{OPh})_3]_4$

	Without extra $\text{P}(\text{OPh})_3$	With extra $\text{P}(\text{OPh})_3$
1-Hexene	Formation of hexane: zeroth order in substrate first order in $p(\text{H}_2)$ Formation of 2-hexene: approximately zeroth order in substrate zeroth order in $p(\text{H}_2)$	Formation of hexane: first order in substrate less than first order in $p(\text{H}_2)$ Formation of 2-hexene: first order in substrate
Allylbenzene	Formation of propylbenzene: induction period Formation of methylstyrene: zeroth order in substrate zeroth order in $p(\text{H}_2)$	Formation of propylbenzene: zeroth order in substrate first order in $p(\text{H}_2)$ Formation of methylstyrene: less than first order in substrate zeroth order in $p(\text{H}_2)$

zene as the substrates in chloroform solution and varied the hydrogen pressure (0.2, 1.0, 5.0 or 10.0 atm partial pressure; see Section 5) and the concentration of triphenylphosphite (zero, one or three extra added equivalents). The concentration of the catalyst was 1.5 mM and the substrate-to-metal ratio was 2000 to 1. The progress of the reaction was followed by gas chromatography (GC).

The catalyst displayed a totally different reactivity after adding extra triphenylphosphite and behaved differently towards the two substrates. The formation of the hydrogenated products vs. time for the different situations is depicted in Fig. 3 and the observations are summarized in Table 1.

Without the addition of extra phosphite ligand the formation of hexane is zero order in substrate and first order in hydrogen pressure (Fig. 3(a)). Above 5 atm the pressure dependence of the rate is no longer linear and declines. The isomerization reaction, giving *Z*- and *E*-2-hexene, is almost a zero-order process and independent of the hydrogen pressure. Only the *Z*-isomer is hydrogenated to hexane. No 3-hexene is formed until all the 1-hexene has reacted. In the case of allylbenzene the rate of hydrogenation increases after an initial induction

Table 2
Zero-order rate constants for the hydrogenation and isomerization of 1-hexene and allylbenzene with $\text{HRh}[\text{P}(\text{OPh})_3]_4$ without additional triphenylphosphite present ^a

	$p(\text{H}_2)$ (atm)	$k_0 \times 10^4$ (M s^{-1})	
		Hydrogenation	Isomerization
1-Hexene	0.2	0.5	3.1
	1	1.1	3.1
	5	4.8	3.4
	10	5.9	3.4
Allylbenzene	5	$\approx 4.6^b$	0.9
	10	3.1	0.9

^a Conditions: [catalyst] = 1.5 mM; [substrate] = 3 M; $T = 25^\circ\text{C}$; solvent, chloroforms.

^b After an induction period of approximately 30 min.

period to the same value as observed for the 1-hexene hydrogenation. No specific dependence of the pressure can be derived from the data (Fig. 3(c)). The isomerization reaction, resulting in *E*- β -methylstyrene (no *Z*-isomer is observed), is zero order in both substrate and the hydrogen pressure. The observed zero-order rate constants are summarized in Table 2. The values are corrected for the hydrogenation of the isomerized products (see Section 5).

When extra equivalents of triphenylphosphite are added to the reaction mixture, both the hydrogenation and the isomerization of 1-hexene become first order with respect to the substrate concentration (Fig. 3(b)). The order in hydrogen pressure is smaller than one for the hydrogenation reaction. The observed rate constants for the formation of hexane and 2-hexene as well as the product composition in the presence of one and three equivalents of additional $\text{P}(\text{OPh})_3$ are presented in Table 3.

In the presence of additional phosphite the hydrogenation of allylbenzene is zero order in substrate and

Table 3
First-order rate constants and selectivities for the hydrogenation and isomerization of 1-hexene with $\text{HRh}[\text{P}(\text{OPh})_3]_4$ in the presence of additional $\text{P}(\text{OPh})_3$ ^a

$p(\text{H}_2)$ (atm)	Hydrogenation		Isomerization	
	Selectivity (%)	$k_1 \times 10^5$ (s^{-1})	Selectivity ^b (%)	$k_1 \times 10^5$ (s^{-1})
One equivalent of $\text{P}(\text{OPh})_3$				
0.2	64.4	4.2	35.6	1.8
1	81.4	5.2	18.6	5.2
5	90.8	17.3	9.2	18.2
10	93.3	22.3	6.7	21.2
Three equivalents of $\text{P}(\text{OPh})_3$				
0.2	66.6	1.3	33.4	1.3
1	78.7	2.5	21.3	2.5
5	91.6	7.2	8.4	7.3
10	93.8	7.5	6.2	6.8

^a Conditions: see Table 2.

^b Total amount of *Z*- and *E*-2-hexene; no 3-hexene was formed.

Table 4

Zero-order rate constants for the hydrogenation of allylbenzene with $\text{HRh}[\text{P}(\text{O}Ph)_3]_4$ in the presence of an additional equivalent of $\text{P}(\text{O}Ph)_3$ ^a

$p(\text{H}_2)$ (atm)	Hydrogenation		Isomerization
	Amount (%)	$k_0 \times 10^4$ (M s^{-1})	Amount (%)
5	89.0	1.0	11.0
10	90.0	1.9	10.0

^a Conditions: see Table 2.

first order in hydrogen pressure (Fig. 3(d)). The isomerization reaction has an order less than one and is independent of $p(\text{H}_2)$. The zero-order rate constants for the hydrogenation of allylbenzene and the product composition in the presence of one extra equivalent of $\text{P}(\text{O}Ph)_3$ are listed in Table 4.

When substrate was added to the catalyst no intermediates could be observed by ¹H NMR spectroscopy and in the ³¹P NMR spectrum only the signal of $[\text{HRh}[\text{P}(\text{O}Ph)_3]_4]$ was visible. Most of the reactions in Scheme 1 are equilibrium reactions and apparently under the conditions of our experiments they are far to the side of $[\text{HRh}[\text{P}(\text{O}Ph)_3]_4]$. Also in the presence of a large excess of substrate the ³¹P NMR spectrum remained unchanged.

3.2. Discussion

It is very plausible to assume that the first step in the hydrogenation and isomerization reactions of the alkenes is the formation of HRhL_3 ($\text{L} = \text{P}(\text{O}Ph)_3$) by dissociation of a phosphite ligand according to



This generates a free coordination site at the rhodium center. The importance of such a site is known from catalytic hydrogenation experiments with the corre-

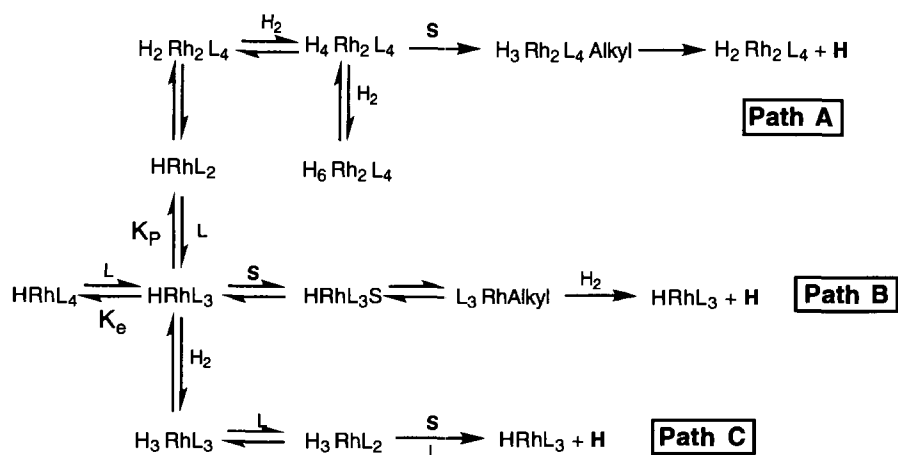
sponding cobalt complexes. Rapid conversions are observed with $[\text{HCo}[\text{P}(\text{O}Ph)_3]_3(\text{CH}_3\text{CN})]$, whereas $[\text{HCo}[\text{P}(\text{O}Ph)_3]_4]$ is essentially inert [7b]. It is known that also the phosphine complex $[\text{HRh}(\text{PPh}_3)_4]$ readily dissociates one of its ligands in solution. Depending on the type of the phosphine a second dissociation also takes place to a certain extent [23]:



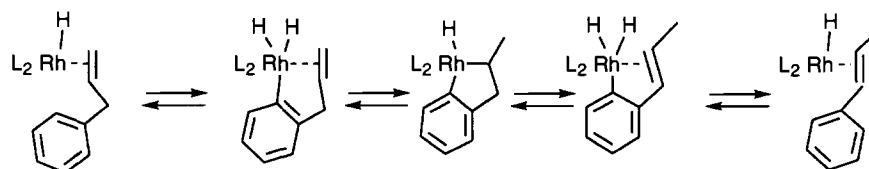
In our case the still rather crowded rhodium-phosphite complex HRhL_3 can undergo three processes: reaction with alkene, reaction with hydrogen, and further dissociation to HRhL_2 (Scheme 2). When an excess of $\text{P}(\text{O}Ph)_3$ is present, the equilibrium concentration of HRhL_2 will be negligible. In the following the equilibrium involving the orthometallation reaction (Scheme 1) do not need to be considered because the reactions are carried out under hydrogen pressure.

The kinetic data for the hydrogenation of 1-hexene to hexane (Tables 1 and 2) imply that, without extra phosphite present, the catalyst first reacts with hydrogen, resulting in an intermediate that can be represented as $\text{L}_n\text{Rh}_m\text{H}_{m+2}$. The fact that the rate of hydrogenation of allylbenzene under these conditions eventually reaches the same value as that observed for 1-hexene (Table 2) suggests that for this substrate a similar mechanism is operative. In the presence of extra $\text{P}(\text{O}Ph)_3$ the data for the hydrogenation of 1-hexene (Table 3) indicate that first coordination of the substrate takes place, giving the species $\text{L}_n\text{Rh}_m\text{H}_m(\text{alkene})$. In contrast with this, the data for the hydrogenation of allylbenzene (Table 4) point to a process that starts with oxidative addition of hydrogen.

A reaction scheme with only one type of catalytic species cannot explain all the kinetic data. We therefore postulate that without extra $\text{P}(\text{O}Ph)_3$ the actual catalyst is a dimeric species $[(\text{HRhL}_2)_2]$, reported by Muetterties and coworkers [6a,24]. This species could be formed



Scheme 2. Proposed reaction mechanism for the hydrogenation and isomerization of olefins by $\text{HRh}[\text{P}(\text{O}Ph)_3]_4$. The substrate is represented as S and the hydrogenation products as H .



Scheme 3.

by dimerization of the 14-electron complex $[\text{HRhL}_2]$ (see Scheme 2, path A). For this mechanism an order in catalyst smaller than one should be observed. We were not able to confirm this because the hydrogenation reaction was very sensitive to the presence of small concentrations of $\text{P}(\text{OPh})_3$ and the purity of the starting complex. The complex $[\{\text{HRh}[\text{P}(\text{O}^{-1}\text{C}_3\text{H}_6)_3]_2\}]$ reported by Muetterties and coworkers is known to be a very powerful hydrogenation catalyst for 1-hexene with turn-overs up to 2 s^{-1} at $p(\text{H}_2) = 1 \text{ atm}$ [6a]. This is much larger ($40\,000\times$) than the turn-over numbers displayed by the monomeric catalyst (e.g. see Table 3; one equivalent of $\text{P}(\text{OPh})_3$; $p(\text{H}_2) = 1 \text{ atm}$). Therefore it is likely that, without additional phosphite present, the hydrogenation route predominantly goes via path A.

The decrease in the hydrogenation rates at higher pressures can be explained by oversaturation of the dimer complex with dihydrogen. Possibly, a second molecule of hydrogen is oxidatively added to $\text{H}_4\text{Rh}_2\text{L}_4$, forming the d_6-d_6 binuclear metal complex $\text{H}_6\text{Rh}_2\text{L}_4$, which is coordinatively saturated and therefore expected to be inactive (Scheme 2, path A). In the case of allylbenzene at $p(\text{H}_2) = 10 \text{ atm}$ this competitive reaction with hydrogen is even preferred above coordination of the alkene.

The amount of isomerized products obtained during the catalytic reactions without additional $\text{P}(\text{OPh})_3$ is considerable. As the hydrogenolysis of the alkyl metal complex normally is a very fast process [2], we believe that a different metal complex is responsible for the isomerization reaction. Possibly, this reaction proceeds via a π -allylic complex which is formed by the oxidative addition of alkene to undimerized HRhL_2 . An alternative pathway for the isomerization of allylbenzene is by way of orthometallation as is shown in Scheme 3.

As during the catalytic reactions no intermediates could be detected by NMR and only the signal of $\text{HRh}[\text{P}(\text{OPh})_3]_4$ was observed, we may conclude that the equilibrium constant K_e (Scheme 2) is small. Therefore it is reasonable to assume that the addition of one or three equivalents of $\text{P}(\text{OPh})_3$ will hardly influence the equilibrium defined by this K_e . It will, however, completely inhibit the dissociation of a second phosphite ligand (equilibrium K_p), blocking the formation of the dimer $\text{H}_2\text{Rh}_2\text{L}_4$. Therefore, when extra phosphite is present, the hydrogenation will merely have to proceed via a monomeric rhodium complex.

In the case of hydrogenation with the monomeric catalyst the size of the substrate is probably decisive for the reaction path. 1-Hexene is small enough to coordinate to the bulky HRhL_3 complex. The observed first-order dependence of the reaction rate on the substrate concentration can be explained by assuming a pre-equilibrium in which alkene is involved (Scheme 2, path B). Since the first-order rate constants for the hydrogenation and isomerization of 1-hexene have the same values we may conclude that these reactions go via a common intermediate. Most probably the isomerization products arise from a β -elimination reaction occurring at the rhodium alkyl complex. The fact that the amount of $\text{P}(\text{OPh})_3$ has no influence on the ratio of hydrogenated and isomerized product is consistent with the supposition that coordination of the substrate is the rate-determining step of the reaction.

Our kinetic data indicate that the rhodium center in HRhL_3 is too shielded to accommodate the relatively bulky allylbenzene. The reaction sequence for this alkene most probably involves the rate-determining oxidative addition of hydrogen to HRhL_3 , giving H_3RhL_3 (Scheme 2, path C). The subsequent dissociation of a ligand may now be facilitated. The absolute rate of the conversion of allylbenzene by this hydride pathway is slower than that of 1-hexene (see Fig. 2 and Table 4).

4. Conclusion

Without additional phosphite present, we propose that the actual catalyst for the hydrogenation of alkenes is a trace amount of the dimeric complex $[\{\text{HRh}[\text{P}(\text{OPh})_3]_2\}]_2$, the catalyst of Muetterties and coworkers, which is much more active than the monomeric catalyst $[\text{HRh}[\text{P}(\text{OPh})_3]_3]$. After the addition of $\text{P}(\text{OPh})_3$ the dimerization reaction is blocked and a monomeric complex is responsible for the hydrogenation. With a small substrate such as 1-hexene the alkene pathway is preferred (Scheme 2, path B) and the functioning of the catalyst resembles that of the phosphine catalyst $[(\text{solvent})_2\text{Rh}^+(\text{PR}_3)_2]$. Apparently, because of the electron-withdrawing property of the π -acidic phosphite ligands, the rhodium center in the neutral hydride complex $\text{HRh}[\text{P}(\text{OPh})_3]_n$ is electronically comparable with that in the ionic phosphine complex. However, because of this π acidity the dissociation of ligands is unfavorable, preventing reaction with more bulky substrates.

Therefore in the latter case the hydride pathway is followed (Scheme 2, path C), and the catalyst acts analogous to the neutral complex $[\text{CIRh}(\text{PPh}_3)_3]$. Thus because of the properties of the phosphite ligands the monomeric phosphite catalyst described in this paper displaces a character intermediate between those of the neutral and ionic rhodium phosphine catalysts.

The poor electron density on the rhodium atom in combination with the restricted accessibility of the metal center makes this catalyst based on phosphite ligands unsuitable for reaction with less donating and sterically hindered substrates. In line with this we observed no hydrogenation of methyl α -acetylaminocinnamate, not even at a hydrogen pressure of 10 atm [25].

5. Experimental section

5.1. Reagents and solvents

Unless otherwise indicated, commercial materials were used as received. Ethanol and methanol were distilled under a nitrogen atmosphere from their corresponding sodium salts. Dichloromethane was distilled from LiAlH_4 . Chloroform and chloroform- d_1 were distilled from phosphorus pentoxide. All solvents were stored on molecular sieves under an inert atmosphere. Benzene was distilled from sodium. Triphenylphosphite was distilled prior to use. 1-Hexene and allylbenzene were distilled from sodium and filtered over basic alumina prior to use to remove the hydroperoxides.

5.2. Apparatus

^1H NMR spectra were recorded on Bruker WH-90, Bruker WM-200 and Bruker AM-400 instruments. Chemical shifts δ are reported downfield from internal $(\text{CH}_3)_4\text{Si}$. Abbreviations used are as follows: s, singlet; d, doublet; qu, quintet; m, multiplet; br, broad. ^{31}P NMR spectra were recorded on Bruker WM-200 and Bruker AM-400 instruments. Chemical shifts δ are reported downfield from external $\text{OP}(\text{OMe})_3$. Mass spectra were recorded on a VG 7060E instrument. Elemental analyses were determined with a Carlo Erba Ea 1108 instrument. For thin layer chromatography, Merck Silica Gel 60 F_{254} plates were used. The hydrogenation and isomerization reactions were monitored on a Varian 3700 gas chromatograph with flame ionization detector. 1-Hexene and its reaction products were separated on a CP PLOT fused silica Al_2O_3 -KCl capillary column (50 m \times 0.22 mm inside diameter; 180°C isoth.). Allylbenzene and its reaction products were separated on a CP-SIL 5CB capillary column (25 m \times 0.25 mm inside diameter; df, \neq 0.12 μm ; temp. prog.). The detector signal was integrated with the help of a HP 3390A integrator.

5.3. $\text{HRh}[\text{P}(\text{OPh})_3]_4$ (2)

Under an inert atmosphere, 1 g (3.2 mmol) of $\text{P}(\text{OPh})_3$ was added to a cooled solution (0°C) of 0.3 g (1.14 mmol) of $\text{RhCl}_3 \cdot 8\text{H}_2\text{O}$ in 10 ml of degassed ethanol. After 1 min the dark color disappeared and the reaction mixture became turbid. Subsequently, 0.12 g (3.2 mmol) of sodium borohydride in 10 ml of ethanol was slowly added. Half-way this addition another 0.8 g (2.6 mmol) of $\text{P}(\text{OPh})_3$ was added. The mixture was stirred for 2 h and allowed to warm up to room temperature. The formed off-white precipitate was filtered off, washed with cold ethanol and dried under vacuum. The product was extracted from the solid material with dichloromethane. The volume of the solution was reduced to about 3 ml and added dropwise to 80 ml of dry methanol. The precipitate was filtered off, washed with cold methanol and dried under vacuum, yielding 1 g (66%) of $\text{HRh}[\text{P}(\text{OPh})_3]_4$ as a white solid. ^{31}P NMR (80 MHz, CDCl_3): δ 127.6 (dd, $J_{\text{Rh-P}} = 229$ Hz, $J_{\text{P-H}} = 44$ Hz) ppm. ^1H NMR (200 MHz, CDCl_3): δ 7.15–6.90 (m, 42H, ArH *meta* and *para*), 6.9–6.7 (m, 18 H, ArH *ortho*), –11.0 (dqu, 1H, $J_{\text{H-P}} = 44$ Hz, $J_{\text{H-Rh}} = 7$ Hz) ppm. Anal. Found: C, 64.09; H, 4.29. $\text{C}_{72}\text{H}_{61}\text{O}_{12}\text{P}_4\text{Rh}$ Calc.: C, 64.29; H, 4.57%.

5.4. Deuterium exchange

A solution of 50 mg of $\text{HRh}[\text{P}(\text{OPh})_3]_4$ in 10 ml of CDCl_3 was stirred for 2 h under a deuterium pressure of 5 atm. ^{31}P NMR (80 MHz, CDCl_3): δ 127.8 (d, $J_{\text{Rh-P}} = 229$ Hz, $J_{\text{P-D}} = 5.4$ Hz, $J_{\text{Rh-D}} = 0.5$ Hz) ppm. ^1H NMR (200 MHz, CDCl_3): δ 7.40–6.90 (m, ArH *meta* and *para*) ppm.

5.5. $[\text{P}(\text{OPh})_3]_3 \overline{\text{Rh}(\text{I})}(\text{o-C}_6\text{H}_4\text{O})\text{P}(\text{OPh})_2$ (4)

This complex was prepared in two ways: (A) by refluxing $\text{HRh}[\text{P}(\text{OPh})_3]_4$ in hexane for 5 min [15] and (B) by a modified literature procedure [12a]. First tris(triphenylphosphite) rhodium(I) chloride (5) was prepared by adding 0.42 g (1.4 mmol) of $\text{P}(\text{OPh})_3$ to a suspension of 0.1 g (0.4 mmol) of $(\text{acac})\text{Rh}(\text{CO})_2$ in 15 ml of dichloromethane and subsequently passing a stream of dry hydrochloric acid through the solution for 5 min. The mixture was concentrated and the product was dissolved in 15 ml of benzene. To this solution was added 0.4 g (1.2 mmol) of a solution of MeMgCl in tetrahydrofuran (22%). The reaction mixture was stirred for 3 h and evaporated to dryness. The main signals in the ^{31}P NMR spectrum of the products obtained by method (A) as well as method (B) were attributed to 4 (see text and Fig. 1).

5.6. Hydrogenation of 1-hexene

In a 50 ml glass vessel, 13.5 mg (10 μmol) of the catalyst $\text{HRh}[\text{P}(\text{OPh})_3]_4$ was dissolved in 4.2 ml of

chloroform. The vessel was placed in an autoclave and 2.5 ml (20 mmol) of 1-hexene was added, resulting in concentrations of 1.5 mM catalyst and of 3 M 1-hexene. The autoclave was evacuated quickly and refilled twice with argon. Finally, a hydrogen gas overpressure of 0.2, 1.0, 5.0 or 10 atm was applied. The reaction was followed at room temperature while stirring. Samples were taken by opening a valve under a stream of argon. The reaction was stopped by rapidly condensing the reaction products into a micro cold trap. Control experiments indicated that by this procedure no change in the product ratio took place.

5.7. Hydrogenation of allylbenzene

The same procedure as described for 1-hexene was followed using 13.5 mg (10 μ mol) of $\text{HRh}[\text{P}(\text{OPh})_3]_4$ in 4.0 ml of chloroform and 2.66 ml (20 mmol) of allylbenzene. In this case the samples were frozen in liquid nitrogen to stop the reaction.

5.8. Data processing

For all the components in the reaction calibrations with regard to an internal standard were made. The gas chromatography calibration standard for hexene was pentane and that for allylbenzene was toluene. A collective calibration was made for the mixture of isomerized hexenes (*Z*- and *E*-, and 2- and 3-hexene). The integrated areas from the recorder were multiplied by the slopes of the corresponding calibration curves and afterwards renormalized to 100%.

The hydrogenated products were made independently by stirring the substrate overnight in acetic acid with a catalytic amount of palladium on carbon under a hydrogen pressure of 10 atm. The isomerized products were prepared by stirring the corresponding substrate overnight in methanol with a catalytic amount of palladium on carbon and a drop of concentrated hydrochloric acid under argon atmosphere.

The zero-order rate constants for the reactions without additional $\text{P}(\text{OPh})_3$ (Table 2) were corrected for the hydrogenation of the isomerization products. The contribution of this reaction to the total amount of hydrogenated product varied from 30% at a hydrogen pressure of 0.2 atm to 2% at a hydrogen pressure of 10 atm (see Fig. 3(a)). To this end the slope of the hexane formation curve after all the substrate had reacted was subtracted from the slope of this curve before that point and added to the slope of the isomerized products.

The first-order rate constants for the reactions with extra $\text{P}(\text{OPh})_3$ (Table 3) were obtained as follows. The maximum amounts of hydrogenated and isomerized products were determined by extrapolation of the straight lines, obtained by plotting the hexane concentration $[\text{H}]$ and the sum of 2- and 3-hexene concentrations $[\text{I}]$ vs.

the 1-hexene concentration $[\text{S}]$, to the point $[\text{S}] = 0\%$, corresponding to $[\text{H}] = [\text{H}]_{\text{max}}$ and $[\text{I}] = [\text{I}]_{\text{max}}$. The rate constants were derived from the slope of $\ln\{1 - ([\text{H}]/[\text{H}]_{\text{max}})\}$ and $\ln\{1 - ([\text{I}]/[\text{I}]_{\text{max}})\}$ vs. time plots.

Acknowledgment

We thank Shell Research BV for the grant that made this research possible.

References

- [1] B.R. James, *Homogeneous Hydrogenation*, Wiley, New York, 1973.
- [2] J.P. Collman, L.S. Hegeudus, J.R. Norton and R.G. Finke, *Principles and Applications of Organotransition Metal Chemistry*, University Science Books, Mill Valley, CA, 2nd edn., 1987.
- [3] (a) J.A. Osborn, F.H. Jardine, and G. Wilkinson *J. Chem. Soc. A*, (1966) 1711; (b) J. Halpern, T. Okamoto and A. Zakhariiev, *J. Mol. Catal.*, 2 (1976) 65; (c) J. Halpern, *Inorg. Chim. Acta*, 50 (1981) 11.
- [4] (a) J. Halpern, *Science*, 217 (1982) 401; (b) J. Halpern, D.P. Riley, A.S.C. Chan; (c) J.J. Pluth, *J. Am. Chem. Soc.*, 99 (1977) 8055; A.S.C. Chan; (d) J. Halpern, *J. Am. Chem. Soc.*, 102 (1980) 838.
- [5] R.A. Sanchez-Delgado and D.L. DeOchoa, *J. Mol. Catal.*, 6 (1979) 303.
- [6] (a) A.J. Sivak and E.L. Muetterties, *J. Am. Chem. Soc.*, 101 (1979) 4878; (b) L.S. Stuhl, M. Rakowski DuBois, F.J. Hirsekorn, J.R. Bleeke, A.E. Stevens and E.L. Muetterties, *J. Am. Chem. Soc.*, 100 (1978) 2405; (c) E.L. Muetterties and J.R. Bleeke, *Acc. Chem. Res.*, 12 (1979) 324.
- [7] (a) L.W. Gosser, *Inorg. Chem.*, 14 (1975) 1453; (b) L.W. Gosser, *Inorg. Chem.*, 15 (1976) 1348.
- [8] H.K.A.C. Coolen, P.W.N.M. van Leeuwen, R.J.M. Nolte, *Angew. Chem.*, 104 (1992) 906; *Angew. Chem., Int. Edn. Engl.*, 104 (1992) 905.
- [9] (a) J.J. Levison and S.D. Robinson, *J. Chem. Soc., Chem. Commun.*, (1968), 1045; (b) J.J. Levison and S.D. Robinson in *Inorganic Syntheses*, Vol. XIII, Wiley, New York, 1972, p. 105.
- [10] A.M. Trzeciak and J.J. Ziolkowski, *Transition Met. Chem.*, 12 (1987) 408.
- [11] (a) F.W. Hoffmann, R.J. Ess and R.P. Usinger, *J. Am. Chem. Soc.*, 78 (1956) 5817; (b) D.H. Gerlach, W.G. Peet and E.L. Muetterties, *J. Am. Chem. Soc.*, 94 (1972) 4545.
- [12] (a) E.K. Barefield and G.W. Parshall, *Inorg. Chem.*, 11 (1972) 964; (b) G.W. Parshall, W.H. Knoth and R.A. Schunn, *J. Am. Chem. Soc.*, 91 (1969) 4990; (c) R. van Eldik, S. Aygen, H. Kelm, A.M. Trzeciak and J.J. Ziolkowski, *Transition Met. Chem.*, 10 (1985) 167; (d) A.M. Trzeciak and J.J. Ziolkowski *Transition Met. Chem.*, 10 (1985) 385; (e) G. Pilloni, G. Zotti and M. Martelli, *J. Electroanal. Chem.*, 63 (1975) 424; (f) S. Aygen and R. van Eldik, *Organometallics*, 6 (1987) 1080.
- [13] M.I. Bruce, *Angew. Chem., Int. Edn. Engl.*, 16 (1977) 73.
- [14] (a) L.M. Haines, *Inorg. Nucl. Chem. Lett.*, 5 (1969) 399; (b) L.M. Haines, *Inorg. Chem.*, 9 (1970) 1517; (c) L.M. Haines, *Inorg. Chem.* 10 (1971) 1693; (d) R. Uson, P. Lahuerta, J. Reyes and L.A. Oro, *Transition Met. Chem.*, 4 (1979) 332.
- [15] M. Preece, S.D. Robinson and J.N. Wingfield, *J. Chem. Soc., Dalton Trans.*, (1976) 613.
- [16] W. Keim, *J. Organomet. Chem.*, 14 (1968) 179.
- [17] *geNMR V3.4 (1989–1993)*, *NMR simulation package*, Ivory-Soft®, Amsterdam, 1989–1993.

- [18] P.E. Garrou, *Chem. Rev.*, **81** (1981) 229.
- [19] P.W.N.M. van Leeuwen, G.J.H. Buisman, A. van Rooy and P.C.J. Kamer, *Recl. Trav. Chim. Pays-Bas*, **113** (1994) 61.
- [20] (a) P. Meakin, E.L. Muetterties and J.P. Jesson, *J. Am. Chem. Soc.*, **94** (1972) 5271; (b) E.M. Hyde, J.R. Swain, J.G. Verkade and P. Meakin, *J. Chem. Soc., Dalton Trans.*, (1976) 1169.
- [21] R.S. Berry, *J. Chem. Phys.*, **32** (1960) 933. In this article, Berry acknowledges the contribution of Dr. F.T. Smith who first pointed out the existence of a pseudorotation operation in a trigonal bipyramid.
- [22] (a) K.C. Dewirst, W. Keim and C.A. Reilly, *Inorg. Chem.*, **7** (1968) 546; (b) S.H. Strauss and D.F. Shriver, *Inorg. Chem.*, **17** (1978) 3069; (c) S.H. Strauss, S.E. Diamond, F. Mares and D.F. Shriver, *Inorg. Chem.*, **17** (1978) 3064.
- [23] (a) J. Hjortkjaer, *Adv. Chem. Ser.*, **132** (1973) 133; (b) D.E. Budd, D.G. Holah, A.N. Hughes and B.C. Hui, *Can. J. Chem.*, **52** (1974) 775.
- [24] V.W. Day, M.F. Fredrich, G.S. Redy, A.J. Sivak, W.R. Pretzer and E.L. Muetterties, *J. Am. Chem. Soc.*, **99** (1977) 8091.
- [25] H.K.A.C. Coolen, P.W.N.M. van Leeuwen and R.J.M. Nolte, unpublished results.